

A Transmembrane Form of the Prion Protein in Neurodegenerative Disease

Ramanujan S. Hegde, James A. Mastrianni, Michael R. Scott, Kathryn A. DeFea, Patrick Tremblay, Marilyn Torchia, Stephen J. DeArmond, Stanley B. Prusiner, Vishwanath R. Lingappa*

At the endoplasmic reticulum membrane, the prion protein (PrP) can be synthesized in several topological forms. The role of these different forms was explored with transgenic mice expressing PrP mutations that alter the relative ratios of the topological forms. Expression of a particular transmembrane form (termed ^{Ctm}PrP) produced neurodegenerative changes in mice similar to those of some genetic prion diseases. Brains from these mice contained ^{Ctm}PrP but not PrP^{Sc}, the PrP isoform responsible for transmission of prion diseases. Furthermore, in one heritable prion disease of humans, brain tissue contained ^{Ctm}PrP but not PrP^{Sc}. Thus, aberrant regulation of protein biogenesis and topology at the endoplasmic reticulum can result in neurodegeneration.

PrP is a highly conserved, 35-kD brain glycoprotein essential for the transmission and pathogenesis of several neurodegenerative diseases, such as scrapie, bovine spongiform encephalopathy, Creutzfeldt-Jakob disease (CJD), and Gerstmann-Straussler-Scheinker (GSS) disease (1). Although the normal function of PrP remains unclear, the pathogenesis of prion diseases requires its expression (2–4) and is often accompanied by the accumulation in the brain of an abnormal isoform of PrP (termed PrP^{Sc}). Considerable evidence from biochemical, immunologic, pathologic, and genetic studies argues that PrP^{Sc} is the major, if not only, component of the transmissible prion particle [reviewed in (1)]. Furthermore, the data suggest that PrP^{Sc} is able to propagate itself in the host by stimulating the conversion of normal cellular PrP (termed PrP^C) to PrP^{Sc}, leading to its accumulation (5, 6). Thus, although the exact mechanism of PrP^C to PrP^{Sc} conversion remains unknown, a foundation has been laid for the understanding of prion disease transmission, on which subsequent structural, biochemi-

cal, and cell biological studies can be based.

More enigmatic at the present time is our understanding of the biochemical and cell biological events that form the basis for the pathophysiological progression of neurodegeneration in prion diseases. The role of PrP^{Sc} in the pathologic process leading to neuronal death is currently unclear. The observation of substantial neurodegeneration in the absence of PrP^{Sc} accumulation in some cases of natural and experimental prion disease argues against its accumulation as the sole cause of pathology (7, 8). Conversely, the time course of PrP^{Sc} deposition in the brains of mice expressing low levels of PrP^C does not correlate with the time course of neurodegeneration (9), raising the possibility that PrP^{Sc} is not directly toxic. This possibility is further supported by the demonstration that PrP^{Sc} deposition fails to cause disease in brain tissue lacking PrP^C (2). Thus, although conversion of PrP^C to PrP^{Sc} appears to be central to transmission, other aspects of PrP expression, folding, and trafficking may feature in the pathophysiological mechanisms that ultimately cause disease.

Studies of PrP translocation at the endoplasmic reticulum (ER) membrane have revealed unusual features in its biogenesis. Whereas most glycoproteins are synthesized in a single orientation with respect to the membrane of the ER, PrP synthesized in cell-free translation systems can be found in more than one topologic form (10–13). One form appears to be fully translocated into the ER lumen and hence is termed the secretory form (^{sec}PrP). This topology is consistent with much of what is known

about PrP^C, which is on the cell surface, tethered to the membrane by a glycolipid anchor whose cleavage results in release from cells (14). The remainder of the PrP made at the ER spans the membrane, with regions of the molecule exposed to the cytosol. However, the relation between these multiple topological forms of PrP and neurodegenerative disease has not been established, nor have transmembrane forms of PrP been previously detected in the brain.

Here, we used transgenic mice that express various mutations in PrP to examine the possible role of PrP topology in neurodegeneration. Our data indicate that a specific transmembrane form of PrP (termed ^{Ctm}PrP, see below) can confer severe neurodegeneration in mice with features typical of prion disease. Subsequent analysis of the human neurodegenerative disease caused by the A117V mutation [alanine (A) to valine (V) substitution at position 117] in PrP suggests that its basis lies in increased production of ^{Ctm}PrP at the ER membrane. These findings identify ^{Ctm}PrP as a key component in the pathway of neurodegeneration in a specific human disorder (GSS) and may have important implications for a broader range of neurodegenerative diseases.

PrP topology. The events of secretory and membrane protein biogenesis can be faithfully reconstituted and studied with cell-free translation systems containing ER-derived microsomal membranes (15). Topology of a protein can be assessed by determining whether any regions of the molecule are accessible to proteases added to the outside of the membrane vesicles. Full protection from exogenous protease indicates complete translocation into the ER lumen. Conversely, digestion of certain domains to yield discrete protease-protected fragments indicates a membrane-spanning topology, the exact orientation of which can be clarified by identification of the protected fragments with epitope-specific antibodies. This use of proteases as a probe of topology is distinctly different from the use of proteases as probes of protein conformation (for example, the protease resistance of PrP^{Sc}). Because the topology assay is carried out in the absence of detergent, the protection from protease is due to an intact membrane barrier. In contrast, the assay of PrP conformation by use of proteinase K (PK) is carried out in detergent solution, where only particular conformations of PrP, and not a membrane barrier, can protect it from digestion (16).

Previous analyses of PrP topology have suggested that two distinct forms of PrP can be made at the ER: one that is fully translocated (^{sec}PrP) and one that is transmembrane (10–12). Digestion of the transmembrane form with proteases added to the

R. S. Hegde and K. A. DeFea are in the Department of Physiology, University of California, San Francisco, CA 94143-0444, USA. J. A. Mastrianni, M. R. Scott, P. Tremblay, and M. Torchia are in the Department of Neurology, University of California, San Francisco, CA 94143-0518, USA. S. J. DeArmond is in the Departments of Pathology and Neurology, University of California, San Francisco, CA 94143, USA. S. B. Prusiner is in the Departments of Neurology and Biochemistry and Biophysics, University of California, San Francisco, CA 94143-0518, USA. V. R. Lingappa is in the Departments of Physiology and Medicine, University of California, San Francisco, CA 94143, USA.

*To whom correspondence should be addressed. E-mail: vrl@itsa.ucsf.edu

outside of the membrane yielded two fragments: One is COOH-terminal derived and glycosylated, and the other is NH₂-terminal derived and unglycosylated. These data have been interpreted to indicate that transmembrane PrP chains span the membrane twice, with the NH₂- and COOH-termini of the molecule in the ER lumen, protected from proteases added to the cytosolic side (10, 13). However, the findings described below suggest that the NH₂- and COOH-terminal fragments reflect the existence of two different transmembrane forms of PrP (Fig. 1A). One form, termed C-transmembrane (CtmPrP), has the COOH-terminus in the ER lumen with the NH₂-terminus accessible to proteases in the cytosol. The other form, termed N-transmembrane (NtmPrP), has the NH₂-terminus in the ER lumen with the COOH-terminus accessible to proteases in the cytosol. Both transmembrane forms appear to span the membrane at the same hydrophobic stretch in PrP (roughly residues 110 to 135, previously termed TM1). For this reason, the proteolytic fragments derived from each transmembrane form share a common domain of PrP approximately from residues 105 to 140 (the residues immediately adjacent to the membrane-spanning domain are not digested by protease, perhaps because of steric hindrance by the membrane itself). Thus, both fragments share the epitope for

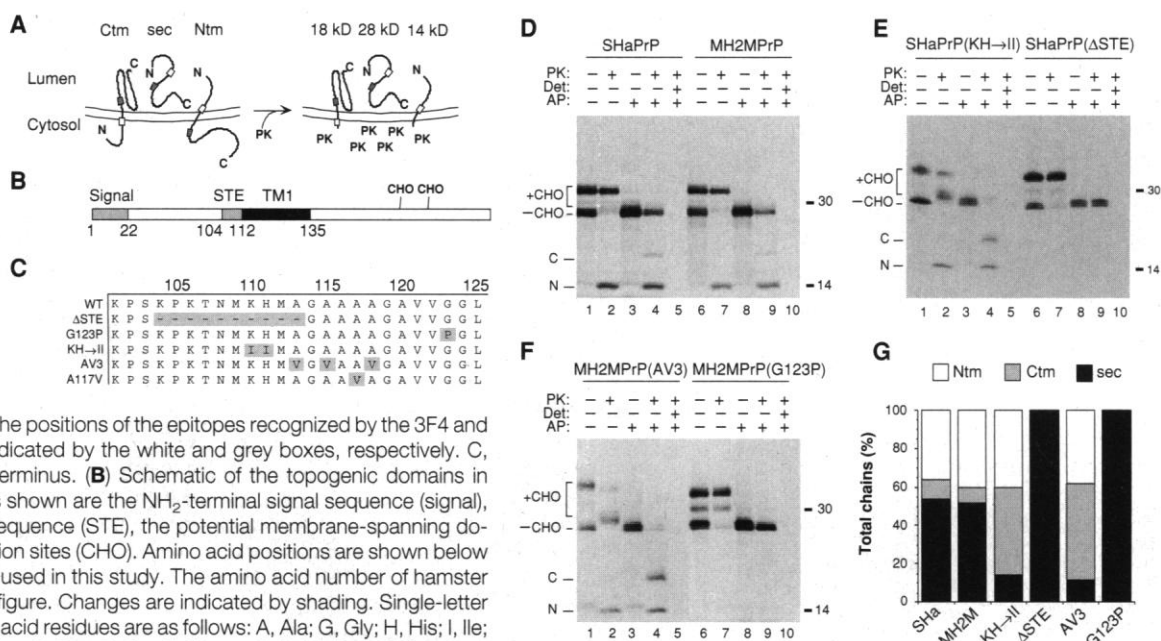
the 3F4 monoclonal antibody (mAb) (to residues 109 to 112), whereas only the COOH-terminal fragment contains the epitope to the 13A5 mAb (to residues 138 to 141). These differences in antibody reactivity, glycosylation, and size allow the NtmPrP and CtmPrP fragments to be clearly distinguished.

Topology-altering mutations in PrP. Synthesis of both transmembrane forms of PrP is dependent on discrete sequences within the PrP coding region (12, 13, 17). Two adjacent domains within PrP (Fig. 1B), the hydrophobic, potentially membrane-spanning stretch from amino acids Ala¹¹³ to Ser¹³⁵ (termed TM1) and the preceding hydrophilic domain [termed STE (for stop transfer effector) and presently narrowed to residues Lys¹⁰⁴ to Met¹¹² (18)], appear to act in concert to generate both transmembrane forms of PrP. No helical structure in this region of PrP has been found by nuclear magnetic resonance studies of recombinant PrPs derived from *Escherichia coli* and studied in an aqueous environment (19–21). Mutations, deletions, or insertions within these domains can alter the relative amounts of each topological form of PrP that is synthesized at the ER (12). Given these complex and unusual features of PrP biogenesis and structure, it seemed plausible to think that its dysregulation may have dramatic consequences for

the physiology of an organism.

To explore this hypothesis, we first identified four mutations within STE-TM1 (shown in Fig. 1C) that greatly alter the ratio of the topological forms when assayed by cell-free translation. Two of these mutations (KH→II and ΔSTE) were engineered into Syrian hamster PrP (SHaPrP), and the other two (AV3 and G123P) were put into MH2MPPrP, a mouse-hamster chimera in which residues 94 to 188 are from hamster PrP (6). We found that the species variation between SHaPrP and MH2MPPrP (differing at eight residues) had little effect on topology (Fig. 1D). However, a comparison of SHaPrP(KH→II) with wild-type SHaPrP showed a marked increase (from ~10 to ~50%) in the relative amount of CtmPrP synthesized, with a concomitant decrease in secPrP (Fig. 1E). The amount of NtmPrP remained essentially unchanged. Similar results were obtained when MH2MPPrP(AV3) was compared with MH2MPPrP (Fig. 1F). In contrast, both SHaPrP(ΔSTE) and MH2MPPrP(G123P) were synthesized exclusively in the secPrP form (Fig. 1, E and F). These results, quantitated and summarized (Fig. 1G), provided the basis for our subsequent examination of the effects of aberrant CtmPrP synthesis in vivo. To do this, we expressed PrP transgenes encoding each of these mutations in mice that lacked the PrP gene [FVB/Prnp^{0/0} (4)]. These mice were

Fig. 1. Analysis of the topology of mutant PrP molecules at the ER membrane with cell-free translation. (A) Schematic of the standard proteolysis assay for PrP topology determination. The three topologic forms of PrP are shown before (left) and after (right) digestion with cytosolically disposed PK. (B) Schematic of the topogenic domains in PrP. Topogenic sequences shown are the NH₂-terminal signal sequence (signal), the stop transfer effector sequence (STE), the potential membrane-spanning domain (TM1), and glycosylation sites (CHO). Amino acid positions are shown below the diagram. (C) Mutations used in this study. The amino acid number of hamster PrP is indicated above the figure. Changes are indicated by shading. Single-letter abbreviations for the amino acid residues are as follows: A, Ala; G, Gly; H, His; I, Ile; K, Lys; L, Leu; M, Met; N, Asn; P, Pro; S, Ser; T, Thr; and V, Val. (D to F) Topology of wild-type and mutant PrP molecules at the ER (39). In vitro-synthesized transcript coding for each PrP construct (indicated above the gels) was used to program a rabbit reticulocyte lysate cell-free translation reaction containing ER-derived microsomal membranes. Where indicated, a competitive peptide inhibitor of glycosylation (AP) was included in the reaction. After translation, samples were either left untreated or digested with PK in the absence or presence of 0.5% Triton X-100 (Det) as indicated above the gel. The positions of unglycosylated (-CHO) and glycosylated (+CHO) PrP species are indicated to the left, and molecular weight markers are indicated to the right. The positions of the NH₂- and COOH-terminal fragments generated by PK digestion of the NtmPrP and CtmPrP forms are indicated at the left of each gel. (G) Quantitative representation (41) of the relative amounts of secPrP (black bars), CtmPrP (gray bars), and NtmPrP (white bars) for each PrP construct analyzed in (D) to (F).



then observed for clinical signs and symptoms and examined for histopathology, and the PrP molecules in their brains were analyzed biochemically for transmembrane topology.

C^mPrP and the development of neurodegeneration. Mice expressing the SHaPrP-(KH→II) transgene [designated Tg[SHaPrP(KH→II)_H], line F1198] developed signs of neurodegeneration. All 29 transgenic mice spanning three generations developed clinical signs of prion disease, including ataxia and paresis (Fig. 2A). In the F2 generation harboring the transgene ($n = 24$), the average age of onset was 58 ± 11 days, with the earliest development of symptoms at 41 days (Fig. 2B). In contrast, none of the nontransgenic littermates exhibited any signs of illness. Neither the FVB/Pmp^{0/0} mice nor FVB/Pmp^{0/0} mice expressing the wild-type SHaPrP transgene [designated Tg-(SHaPrP), line A3922] developed any signs of neurologic dysfunction. Careful quantitation of PrP expression levels demonstrated that Tg[SHaPrP(KH→II)_H] expressed PrP at about half the level seen in the Tg(SHaPrP) mice, indicating that disease was not a trivial consequence of massive overexpression [which has been shown to cause a neuromyopathy at ages of 1 year or more (22)].

Transgenic mice expressing MH2MPrP-(AV3) at high levels also showed neurological signs of illness and death within 2 months (23). Biochemical analyses of mutant PrP in selected ill founder animals (Fig. 3) revealed the expression level to be equal to or lower than that in the brains of Tg-(SHaPrP) mice, again militating against the explanation of overexpression. Thus, similar

Table 1. Mutational analysis of PrP in vitro and in vivo. NA, not applicable.

	C ^m PrP cell free (relative to wild type)	Level of expression (relative to SHa)	Detection of C ^m PrP in brain	Clinical symptoms	Neuropathology in brain	PrP ^{Sc} detection in brain
Wild type	=	4×	-	-	-	-
ΔSTE	<	2.5–3×	-	-	-	-
G123P	<	2×	-	-	-	-
(KH→II) _H	>	2×	+	+	+	-
(KH→II) _L	>	0.25–0.5×	-	-	-	-
AV3	>	2–4×	+	+	+	-
A117V*	>	NA	+	+	+	-

*The A117V mutation is in human PrP, and the data for this mutant derive from analysis in vitro (Fig. 4) or from human brain tissue (Fig. 6B) (26). The data for the other mutants derive from analysis of transgenic mice presented in this paper (Figs. 1 to 3).

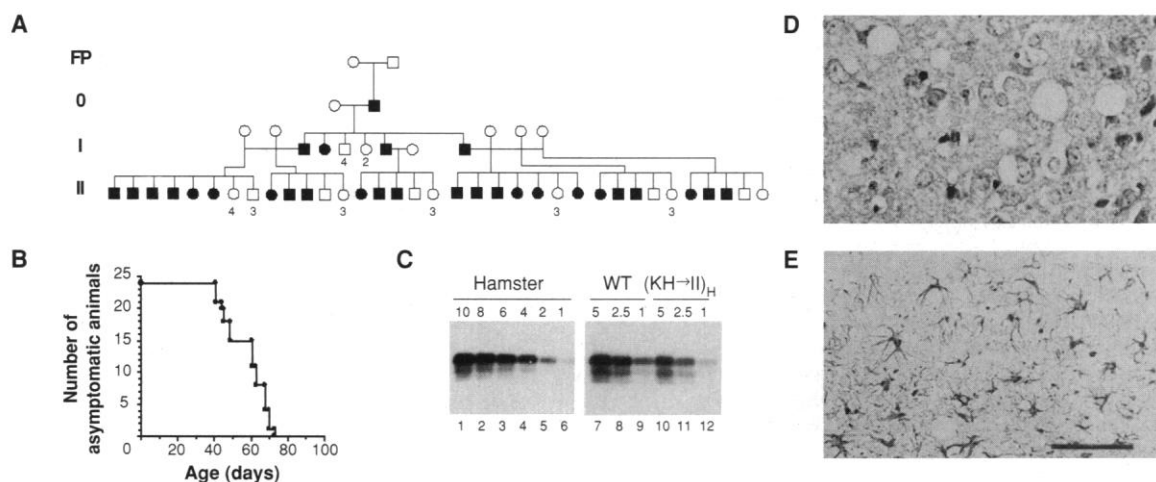
to the KH→II mutation, expression of the AV3 mutation caused a neurodegeneration in mice.

Histopathological examination of brains from ill Tg[SHaPrP(KH→II)_H] mice revealed some neuropathological changes that were similar to those found in scrapie caused by inoculation of animals with prions. These changes included focal vacuolar degeneration of the gray matter neuropil (most pronounced in the hippocampus and piriform cortex; Fig. 2D) and an associated astrocytic gliosis (Fig. 2E). Such pathology was seen in each of the multiple Tg[SHaPrP(KH→II)_H] mice analyzed but was not observed in the brains of normal mice, FVB/Pmp^{0/0} mice, or Tg(SHaPrP) mice. Analysis of ill mice expressing the MH2MPrP(AV3) transgene also revealed neurodegeneration with marked astrocytic gliosis (23). However, unlike with Tg[SHaPrP(KH→II)_H] mice, vacuolar degen-

eration was not consistently observed. Whether this variance in the neuropathology between Tg[SHaPrP(KH→II)_H] and Tg[MH2MPrP(AV3)] mice is due to differences in the level of expression, the age at examination, the species of PrP gene used (SHaPrP versus MH2MPrP), or the location or nature of the mutation itself remains to be determined.

Transgenic mice expressing SHaPrP-(ΔSTE) and MH2MPrP(G123P) were also constructed, and a line with high levels of expression of each [designated Tg[SHaPrP-(ΔSTE)], line F1788, and Tg[MH2MPrP-(G123P)], line D13638] was selected for further study (Table 1). In contrast to mice carrying the KH→II or AV3 mutation in PrP, neither Tg[SHaPrP(ΔSTE)] nor Tg[MH2MPrP(G123P)] mice showed any signs of illness. Furthermore, even at ages substantially beyond the life-span of the Tg[SHaPrP(KH→II)_H] mice, histological

Fig. 2. Production and histological characterization of a transgenic mouse line expressing SHaPrP-(KH→II). (A) Genealogy of the Tg[SHaPrP(KH→II)_H] transgenic line (42). Individuals carrying the transgene are indicated by solid symbols (each of which succumbed to neurodegenerative disease). Open symbols indicate nontransgenic littermates. Males are indicated with a square and females with a circle. Numerals below some symbols indicate multiple individuals represented by that symbol. FP indicates the founding parents, and 0, I and II indicate the founder, F1, and F2 generations, respectively. (B) The F2 transgenic animals ($n = 24$) were observed for signs of neurodegenerative disease, including ataxia and paresis. Plotted on the ordinate axis are the number of asymptomatic animals in the group at any given age (in days). (C) Assessment of the level of expression of Tg[SHaPrP(KH→II)_H] and Tg(SHaPrP). PrP in varying amounts of brain homogenate (amount of total protein in micrograms is indicated above each



lane) from either normal Syrian hamster, Tg(SHaPrP) mouse (WT), or Tg[SHaPrP(KH→II)_H] mouse was detected by immunoblotting with the 13A5 mAb. (D) Hematoxylin and eosin stain of immersion-fixed brain sections (38) from Tg[SHaPrP(KH→II)_H] mice showing mild to moderate vacuolation. (E) Analysis of Tg[SHaPrP(KH→II)_H] mice by immunohistochemical staining of immersion-fixed brain section with antibodies to glial fibrillary acidic protein (38), demonstrating reactive astrocytic gliosis. Scale bar, 50 μ m.

analysis of Tg[SHaPrP(Δ STE)] and Tg-[MH2MPrP(G123P)] mice revealed no neuropathological changes. Taken together with the above findings, these results are suggestive of the notion that favored synthesis in the C^{tm} PrP form, as judged by the cell-free translocation assay, is indicative of the pathogenicity of the PrP mutation in vivo.

The topology of PrP in the brains of these transgenic mice was examined next. For these studies, brains were removed from animals, and intact microsomal membranes, containing PrP among other proteins, were prepared. These intact vesicles were then subjected to protease digestion, and the accessibility of PrP to protease was assessed by immunoblotting. Generation of a proteolytic fragment encompassing the COOH-terminus of PrP argues that these molecules are in the C^{tm} PrP orientation, whereas full protection from protease digestion indicates that the PrP is in the sc PrP orientation. Analysis of the proteolytic fragments was simplified by the removal, just before SDS-polyacrylamide gel electrophoresis (PAGE), of the highly heterogeneous carbohydrate trees with the enzyme PNGase F. This removal allowed us to look for the 18-kD COOH-terminal fragment characteristic of the C^{tm} PrP form, without the complications of heterogeneous electrophoretic migration of variably glycosylated PrP molecules. To

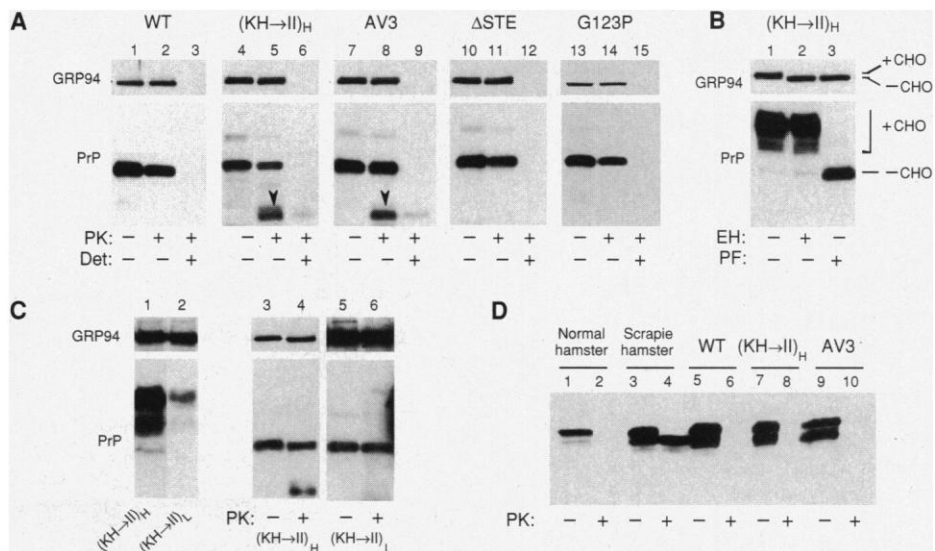
ensure that vesicle integrity was maintained during the proteolysis reaction, we also evaluated the accessibility to protease of GRP94, an ER luminal protein (24).

Only the Tg[SHaPrP(KH \rightarrow II)_H] and Tg[MH2MPrP(AV3)] brain samples contained PrP molecules spanning the membrane, which, after protease digestion in the absence of detergent, produced an 18-kD fragment (Fig. 3A). This fragment produced by protease digestion was determined to be a COOH-terminal fragment of PrP on the basis of its detection with the 13A5 mAb and its observed slower migration on SDS-PAGE as a heterogeneous set of bands if polysaccharides were not removed from PrP before analysis (18). Thus, brains from Tg-[SHaPrP(KH \rightarrow II)_H] and Tg[MH2MPrP(AV3)] mice contained C^{tm} PrP (accounting for ~20 to 30% of the PrP in the microsomes). Similar results were obtained from multiple Tg[SHaPrP(KH \rightarrow II)_H] and Tg[MH2MPrP(AV3)] animals, whereas in no instance was any C^{tm} PrP detected in Tg(SHaPrP), Tg[SHaPrP(Δ STE)], or Tg-[MH2MPrP(G123P)] animals. Taken together, these data indicate that the presence of the C^{tm} PrP form of PrP in the brains of transgenic mice correlates well with observations made with the cell-free translocation system, although the absolute amount of C^{tm} PrP in brain was consistently less than that observed in cell-free assays (see below).

These findings suggest that C^{tm} PrP is involved in the development of spontaneous neurodegenerative disease.

To determine whether the C^{tm} PrP observed in transgenic mice brains had exited the ER, we analyzed the state of maturation of the carbohydrate trees present on PrP. While still in the ER, carbohydrates can be removed efficiently with the enzyme endoglycosidase H (endo H) (25). However, upon transit of proteins to the Golgi apparatus, the sugar trees are trimmed and rendered resistant to endo H and can only be removed with the enzyme PNGase F. We thus determined whether the PrP molecules in brain microsomes (~20 to 30% of which are in the C^{tm} PrP form for Tg[SHaPrP(KH \rightarrow II)_H] and Tg[MH2MPrP(AV3)] had acquired resistance to endo H digestion. As a control, the resident ER protein GRP94 (24), which would not be expected to acquire endo H resistance, was also examined. We found that very little (<2%) of the PrP was digested with endo H, whereas ~100% of the GRP94 in the same sample was digested [Fig. 3B shows that analysis for Tg[SHaPrP(KH \rightarrow II)_H]; identical results were obtained with each of the other transgenic lines (18)]. By contrast, both PrP and GRP94 were digested completely with PNGase F. Thus, nearly all of the PrP, including C^{tm} PrP seen in Tg[SHaPrP(KH \rightarrow II)_H] and Tg[MH2MPrP(AV3)]

Fig. 3. Biochemical characterization of mice expressing mutant PrP transgenes. **(A)** Intact microsomal membranes isolated from the brain tissue (43) of various transgenic mice (as indicated above each gel) were subjected to digestion with PK in the absence or presence of 0.5% Triton X-100 (Det). After completion of the proteolysis reactions, all samples were digested with PNGase F and analyzed by SDS-PAGE and immunoblotting with the 3F4 mAb (lanes 1 to 3, 7 to 9, and 13 to 15) or the 13A5 mAb (lanes 4 to 6 and 10 to 12). The arrowheads in lanes 5 and 8 point to the COOH-terminal proteolytic fragment indicative of the C^{tm} PrP form. In parallel, the blots were also probed with the 9G10 mAb (Stressgen Biotechnologies, Victoria, Canada) to detect GRP94, an ER luminal protein (24). Complete protection of GRP94 in the absence of detergent in each instance indicates that the PK had access to only the outside of the vesicles. **(B)** Microsomal membrane proteins isolated from brain tissue of a Tg[SHaPrP(KH \rightarrow II)_H] transgenic mouse were denatured in 1% SDS and digested with either endo H (EH) or PNGase F (PF), and the samples were analyzed by immunoblotting with 13A5 or 9G10 mAbs to detect PrP and GRP94, respectively. The positions of glycosylated (+CHO) and deglycosylated (-CHO) PrP and GRP94 are indicated. **(C)** Equal amounts of total brain homogenate from Tg[SHaPrP(KH \rightarrow II)_H] (lane 1) and Tg[SHaPrP(KH \rightarrow II)_L] (lane 2) mice were analyzed by protein immunoblotting for PrP (with the 13A5 mAb) and GRP94. Serial dilutions of the Tg[SHaPrP(KH \rightarrow II)_H] sample showed it to contain about fourfold to eightfold more than the Tg[SHaPrP(KH \rightarrow II)_L] sample (44). The topology of Tg[SHaPrP(KH \rightarrow II)_H] (lanes 3 to 4) and Tg[SHaPrP(KH \rightarrow II)_L] (lanes 5 to 6) mice was analyzed as in (A). The amount of PrP that was visualized was



normalized by adjusting the exposure time to the film. Identical results were obtained when the amount of visualized PrP was normalized by adjusting the amount of sample analyzed (18). **(D)** Analysis of transgenic mice for PrP^{Sc}. Ten percent brain homogenates from normal hamster, a hamster sick with experimental scrapie, Tg(SHaPrP) mouse (WT), Tg[SHaPrP(KH \rightarrow II)_H] mouse, or Tg[MH2MPrP(AV3)] mouse were prepared in PBS containing 1% NP-40 and 1% deoxycholate. The samples were either left untreated (odd numbered lanes) or digested with PK (100 μ g/ml) for 60 min at 37 $^{\circ}$ (even numbered lanes) as described previously (45). After termination of the PK reaction with PMSF, samples were analyzed by immunoblotting with the 13A5 mAb.

samples, had exited the ER and resided in a post-ER compartment.

Level of expression modulates C^{tm} PrP and disease. That the percentage of PrP molecules found in the C^{tm} PrP topology in vivo was consistently lower than that found in vitro (compare Fig. 1 with Fig. 3) suggests that cells normally have mechanisms to prevent the accumulation of this potentially pathogenic protein. Thus, the basis for the modest C^{tm} PrP accumulation in brain in the KH \rightarrow II or AV3 mutant may be a combination of overexpression and the severe skew toward C^{tm} PrP synthesis, which together exceed the cell's ability to eliminate or prevent synthesis of C^{tm} PrP. As a result, C^{tm} PrP would accumulate, exit the ER, and trigger disease. If this scenario were the case, then one would predict that lower levels of expression of a C^{tm} PrP-favoring mutant should fall below such a threshold and thus produce only sec PrP. Such mice would be predicted not to get sick despite the mutation in the PrP gene, owing to the absence of C^{tm} PrP.

We explored this idea by first identifying a transgenic line of mice [designated Tg[SHaPrP(KH \rightarrow II)_L], line E12485] expressing the KH \rightarrow II mutation at low levels. This line contained about one-fourth to one-half the level of PrP found in normal Syrian hamster, corresponding to levels \sim fivefold lower than in the Tg[SHaPrP(KH \rightarrow II)_H] mice (Fig. 3C). Upon biochemical examination of the brain, C^{tm} PrP was not detected in Tg[SHaPrP(KH \rightarrow II)_L] mice, with all of the PrP being in the sec PrP form (Fig. 3C). Thus, by decreasing the level of transgene expression by a factor of \sim five, the percentage of PrP in the C^{tm} PrP form was reduced from \sim 30% to undetectable levels, even upon overexposure of the blots, under conditions at which sec PrP was readily detectable. Corresponding to this lack of C^{tm} PrP generation, observations

of the animals from the Tg[SHaPrP(KH \rightarrow II)_L] line have thus far revealed no signs of illness at ages greater than 400 days. This observation is in sharp contrast to the Tg[SHaPrP(KH \rightarrow II)_H] line, which showed both C^{tm} PrP and signs of disease at \sim 60 days of age (Fig. 2B). These data support the hypothesis that generation of C^{tm} PrP leads to neurodegeneration in mice, with the role of the mutation being limited to one of favoring synthesis of C^{tm} PrP.

Spontaneous disease without PrP^{Sc} accumulation. The data thus far suggest that the basis of disease pathogenesis for the KH \rightarrow II and AV3 mutants of PrP is an increase in C^{tm} PrP production. However, given the association of protease-resistant PrP^{Sc} and various prion diseases, one might wonder whether the mutations described predispose toward spontaneous conversion to PrP^{Sc} and whether accumulation of this isoform is the cause of the disease observed. Although further studies will be required to determine whether the spontaneous disease caused by the KH \rightarrow II and AV3 mutations is transmissible, we analyzed brains of the ill transgenic mice for the presence of protease-resistant PrP^{Sc}. We were unable to detect protease-resistant PrP^{Sc} in either the Tg[SHaPrP(KH \rightarrow II)_H] or Tg[MH2MPPrP(AV3)] mice (Fig. 3D) even after overloading the gels. Consistent with these findings, immunohistochemistry of brain sections (after hydrolytic autoclaving) from Tg[SHaPrP(KH \rightarrow II)_H] and Tg[MH2MPPrP(AV3)] failed to detect PrP^{Sc} (18). These data further support the notion that C^{tm} PrP overexpression, and not the accumulation of protease-resistant PrP^{Sc}, causes the neurodegeneration observed in transgenic mice expressing the KH \rightarrow II and AV3 mutations.

C^{tm} PrP and human neurodegenerative disease. Given that the distribution of newly synthesized PrP between transmembrane and secretory topologic forms is readily ma-

nipulated with mutations, we reasoned that there may exist in nature human mutations with similar, but less severe, effects on PrP topology. Such mutations would be likely to cause disease on a more delayed time scale, allowing them to be passed on to the next generation, and would be likely to have a less extreme skew in favor of C^{tm} PrP, when analyzed in cell-free systems. A PrP mutation causing GSS, in which there is an alanine (A) to valine (V) substitution at position 117 (A117V) (26), was a likely candidate for several reasons. First, this mutation lies in the hydrophobic domain (TM1) that is crucial to the biogenesis of the transmembrane forms of PrP (12). Second, the pathological findings in these cases of GSS (26) appear to share some features with mice that become ill because of C^{tm} PrP overexpression. Third, the biochemical examination of brain tissue from these cases of GSS has revealed little, if any, protease-resistant PrP (27, 28). These observations raised the possibility that a mechanism other than PrP^{Sc} accumulation was involved in the pathogenesis of these cases of GSS.

To explore the mechanism by which the A117V mutation may cause disease, we compared the biogenesis in a cell-free system of this mutant PrP with its wild-type counterpart (both of which contained a valine at the polymorphic position 129). Upon examination of the GSS mutant PrP molecule [HuPrP(A117V)], we noticed that it consistently contained higher amounts of the transmembrane forms of PrP than did wild-type HuPrP (Fig. 4A). Quantitative analysis of multiple independent translocation reactions (Fig. 4B) demonstrated that the A117V mutation favored the synthesis of both C^{tm} PrP and N^{tm} PrP, with a concordant decrease of the sec PrP form. Thus, a mutation of PrP in the STE-TM1 region that is associated with human disease showed a relative preference for synthesis of the transmembrane forms of PrP upon expression in cell-free translation systems, consistent with the hypothesis that a transmembrane form of PrP could play a role in GSS.

To explore this idea further, we examined brain tissue from a GSS patient to determine whether in vivo, increased levels of transmembrane forms of PrP could be detected. Unfortunately, assay of protein topology in human brain is problematic because fresh tissue suitable for subcellular fractionation is not readily available. Moreover, frozen specimens do not maintain adequate subcellular architecture, posing yet another obstacle to isolation of intact intracellular membranes that would be suitable for topologic studies. To overcome these obstacles, we developed an alternate assay to distinguish

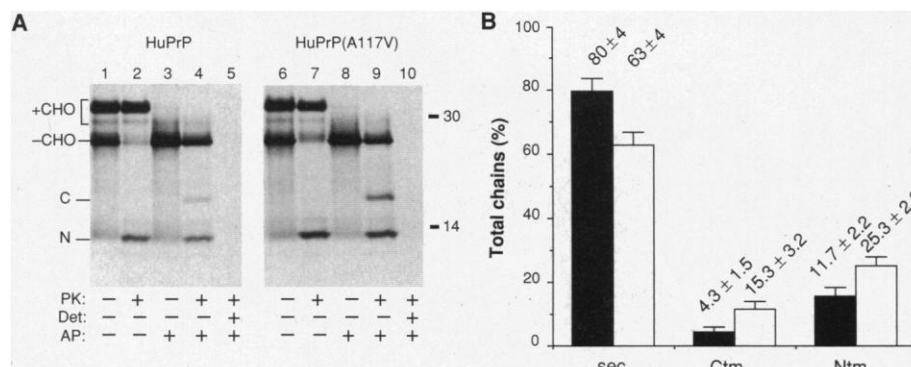


Fig. 4. The A117V mutation in PrP alters the ratio of topological forms synthesized at the ER. (A) HuPrP and HuPrP(A117V) topology at the ER membrane was assessed exactly as in Fig. 1. (B) Data from six experiments performed as in (A) were quantitated to assess the relative amounts of the three topological forms (47) and averaged to obtain a mean \pm SEM (indicated above each bar). The black and white bars represent wild-type and mutant (A117V) PrP, respectively.

the different topological forms of PrP.

We sought to exploit differences in the native conformations that would be expected of the different topologic forms of PrP. Such differences in conformation may be maintained in extracts from frozen brain and would be lost completely only upon denaturation. Differences in tertiary structure are often reflected in the relative accessibility of certain domains of a protein to macromolecular probes such as antibodies or proteases (29). Indeed, an extreme example of this property is the differential sensitivity to PK of PrP^C and PrP^{Sc}, with the latter being highly resistant to digestion (16). To determine whether a similar assay based on differential protease resistance could be used to distinguish the different topological forms of PrP, we digested cell-free translation products of PrP with PK under various conditions (Fig. 5A). One or more nondenaturing detergents were included to solubilize membranes and allow the PK access to all of the PrP molecules in the reaction. We found that although harsh digestion at increased concentrations of PK (at >500 μg/ml) or increased temperature (37°C) could digest completely all topological forms of PrP [but not PrP^{Sc} (16)], a subset of PrP was only partially digested under the milder conditions of PK (250 μg/ml) and 0°C (Fig. 5A). The fragment generated under these conditions comigrated on SDS-PAGE with the protected COOH-terminal domain generated in the standard topology assay.

Digestion of each of the topological mutants of PrP under the same conditions revealed that the generation of the protease-resistant fragment correlated well with the amount of CtmPrP formed: Mutations that increased the relative amount of

PrP in this form (A117V, KH→II, and AV3) resulted in increased generation of the PK-resistant fragment, whereas mutations that abolished synthesis of this form (ΔSTE and G123P) did not yield a PK-resistant fragment (18). As expected, all of the topological forms were completely digested by the harsher treatment under which PrP^{Sc} is able to survive. Thus, at least in the cell-free system, these conditions were able to distinguish ^{sec}PrP and ^{Ntm}PrP from CtmPrP, which could be further distinguished from PrP^{Sc} (Fig. 5B).

To confirm that we could distinguish CtmPrP from both ^{sec}PrP and PrP^{Sc} in frozen brain tissue samples, we performed the assay on samples from transgenic mice in which the distribution of PrP among the topological forms had previously been established. Frozen brain tissue from Tg(SHaPrP), Tg[SHaPrP(KH→II)_L], and Tg[SHaPrP(KH→II)_H] mice was analyzed and compared with products of the standard topology assay performed with intact membranes. We further included as a marker the PrP^{Sc} fragment generated from PK digestion of scrapie-infected hamster brain homogenate. We found that, similar to the results of the standard topology assay, the conformational assay generated a protease-protected fragment only in the Tg[SHaPrP(KH→II)_H] sample (Fig. 6A). Thus, the presence of this COOH-terminal fragment, generated under the mild but not under the harsh digestion conditions, appeared to be diagnostic for the presence of CtmPrP.

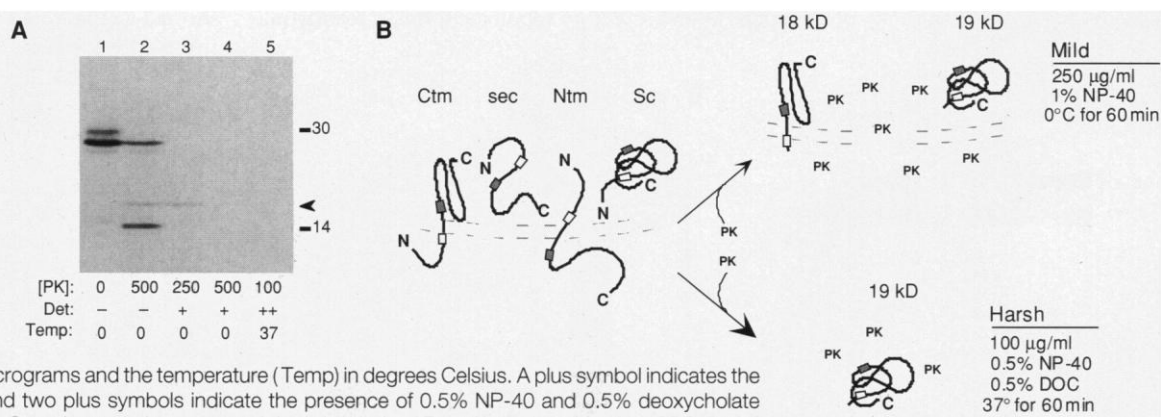
With the ability to analyze frozen brain tissue for the presence of CtmPrP (distinguished from either PrP^C, ^{sec}PrP, or PrP^{Sc}), we were able to ask whether GSS caused by the A117V mutation was due to increased

levels of CtmPrP. Frozen brain tissue from a neurologically normal patient and a GSS patient, taken at autopsy, was analyzed for the presence of CtmPrP and PrP^{Sc} with the appropriate assays. We found comparable levels of PrP in both normal and GSS human brain (Fig. 6B). However, the GSS brain contained increased levels of CtmPrP compared with the normal control (Fig. 6B). By contrast, neither brain had detectable protease-resistant PrP^{Sc} under conditions at which it was readily found in tissue from a sporadic CJD patient (Fig. 6B). These results were independently confirmed by analysis of multiple samples of tissue from the same patient and also with brain tissue from a second patient carrying the same mutation. The lack of accumulation of protease-resistant PrP^{Sc} was also independently confirmed for the second patient (28). Thus, consistent with observations in vitro, the A117V mutation resulted in increased generation of CtmPrP in vivo, suggesting that CtmPrP accumulation is likely to be the cause of at least some of the neuropathological changes seen in these cases of GSS.

A new paradigm for PrP-induced neurodegeneration. Our studies were motivated by the desire to determine the role in prion diseases played by a transmembrane form of PrP that was first identified through the use of cell-free translation-translocation systems (10). The hypothesis that a specific topologic form of PrP, namely CtmPrP, is involved in the development of neurodegeneration is supported in several ways (summarized in Table 1). First, two independent mutations of PrP (KH→II and AV3), which were initially identified by their ability to favor markedly the synthesis of CtmPrP in cell-free systems, caused accel-

Fig. 5. (A) Characterization of topologic forms of PrP by limited PK digestion.

SHaPrP, translated as described in Fig. 1B (with ER-derived microsomal membranes and a competitive peptide inhibitor of glycosylation), was subjected to proteolytic digestion with PK for 60 min under the conditions indicated below each lane. The amount of PK is given in micrograms and the temperature (Temp) in degrees Celsius. A plus symbol indicates the presence of 1% NP-40, and two plus symbols indicate the presence of 0.5% NP-40 and 0.5% deoxycholate (DOC) during the digestion. Samples were immunoprecipitated with the 3F4 mAb and analyzed by SDS-PAGE and autoradiography. The arrowhead indicates the position of a relatively resistant fragment generated upon PK digestion (lane 3) that comigrates with the COOH-terminal fragment derived from CtmPrP (lane 2). The numbers on the right are the molecular weight markers. **(B)** Schematic of limited PK digestion of the various topologic forms of PrP. The three topologic forms of PrP are shown before (left) and after (right) digestion with PK under mild (top) or harsh (bottom) conditions. The approximate sizes of the fragments generated from CtmPrP (18 kD) and PrP^{Sc} (19 kD) are indicated above the diagram. The positions of the epitopes recognized by the 3F4 and 13A5 mAbs are indicated by the white and grey boxes, respectively. The detergent-solubilized membrane is indicated by a dashed line.

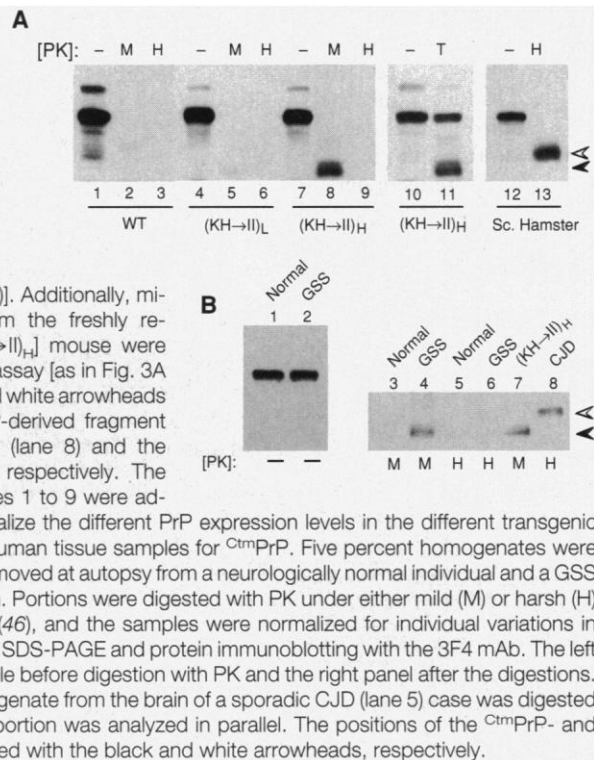


erated spontaneous neurodegeneration and death in transgenic mice. Second, other PrP mutations in the STE-TM1 domain that abolish expression of $C^{tm}PrP$ in cell-free systems (ΔSTE and G123P) did not cause spontaneous disease in transgenic mice. Third, biochemical examination of PrP topology in the brains of transgenic mice expressing pathogenic mutations of PrP revealed the presence of $C^{tm}PrP$ in vivo, whereas this form was not seen in mice expressing a comparable level of wild-type PrP. Fourth, mice expressing the pathogenic KH \rightarrow II mutation at lower levels did not contain $C^{tm}PrP$ (but did contain $secPrP$) in brain and, correspondingly, failed to show signs of disease. Fifth, examination of the brains of ill mice failed to reveal the presence or accumulation of protease-resistant PrP Sc . Finally, a naturally occurring human disease-causing mutation in PrP caused increased $C^{tm}PrP$ formation in vitro and in vivo. Taken together, these data strongly suggest that expression of $C^{tm}PrP$ can cause neurodegeneration.

Several lines of evidence currently indicate that the pathologic processes resulting in $C^{tm}PrP$ -associated neurodegeneration are directly relevant to prion diseases. First, the neuropathology observed in the brains of Tg[SHaPrP(KH \rightarrow II) $_{H}$] and Tg[MH2MPrP(AV3)] is very similar to that observed in several prion diseases (27, 30). Second, the apparent lack of protease-resistant PrP Sc in Tg[SHaPrP(KH \rightarrow II) $_{H}$] and Tg[MH2MPrP(AV3)] mice is not unprecedented in prion disease. Rather, in several inherited prion diseases, certain mutations cause neuropathology despite little detectable PrP Sc (8, 27, 31). Finally, it does not appear that the disease observed in this study is due to nonspecific accumulation of misfolded or aggregated PrP molecules. This conclusion is supported by the observation of nearly all of the $C^{tm}PrP$ being located in a post-ER compartment, a lack of excessive accumulation of PrP (that is, no plaques or other localized deposition of PrP), and a lack of neuropathology characteristic of a storage-type disorder (32). Together, these data support the hypothesis that expression of $C^{tm}PrP$ may be involved in the pathologic process occurring in at least a subset of heritable prion diseases.

At present, the data in this study are suggestive of at least three distinct steps in the pathogenesis of $C^{tm}PrP$ -associated neurodegenerative disease (Fig. 7). The first step is preferential synthesis of $C^{tm}PrP$ over other topological forms at the ER membrane. Second, newly synthesized $C^{tm}PrP$, which may normally be degraded rapidly, exits from the ER. Finally, in a post-ER compartment, $C^{tm}PrP$ is proposed to serve an as yet unknown function to cause, di-

Fig. 6. (A) Characterization of limited digestion of PrP in homogenate from frozen brain. Ten percent homogenate from the frozen brain of either a Tg[SHaPrP] mouse (WT) (lanes 1 to 3), Tg[SHaPrP(KH \rightarrow II) $_{L}$] mouse (lanes 4 to 6), Tg[SHaPrP(KH \rightarrow II) $_{H}$] mouse (lanes 7 to 9), or scrapie (Sc)-infected hamster (lanes 12 and 13) was digested under mild (M) or harsh (H) (or both) conditions [as defined in Fig. 5B (42)]. Additionally, microsomal membranes isolated from the freshly removed brain of a Tg[SHaPrP(KH \rightarrow II) $_{L}$] mouse were analyzed by the standard topology assay [as in Fig. 3A (36)] (lanes 10 and 11). The black and white arrowheads indicate the position of the $C^{tm}PrP$ -derived fragment from the standard topology assay (lane 8) and the PrP Sc -derived fragment (lane 10), respectively. The amounts of sample analyzed in lanes 1 to 9 were adjusted, before SDS-PAGE, to normalize the different PrP expression levels in the different transgenic lines (see Table 1). **(B)** Analysis of human tissue samples for $C^{tm}PrP$. Five percent homogenates were prepared from frozen brain tissue removed at autopsy from a neurologically normal individual and a GSS case containing the A117V mutation. Portions were digested with PK under either mild (M) or harsh (H) conditions as described in Fig. 5B (46), and the samples were normalized for individual variations in starting PrP levels before analysis by SDS-PAGE and protein immunoblotting with the 3F4 mAb. The left panel shows a portion of each sample before digestion with PK and the right panel after the digestions. As a marker for human PrP Sc , homogenate from the brain of a sporadic CJD (lane 5) case was digested under the harsh conditions, and a portion was analyzed in parallel. The positions of the $C^{tm}PrP$ - and PrP Sc -derived fragments are indicated with the black and white arrowheads, respectively.



rectly or indirectly, neurodegeneration.

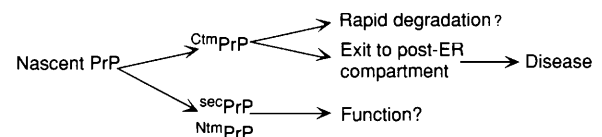
There are three lines of evidence for the first step. First, PrP can be made in more than one topological form in cell-free translation systems [(10–12), and this study]. Second, $C^{tm}PrP$ has now been detected in vivo (Fig. 3A). Finally, PrP topology is dependent on both the amino acid sequence [(12), and this study] and trans-acting factors in the cytosol (13) and in the ER membrane (18). Thus, not only is PrP able to be made in multiple topological forms, but this step appears to be regulated in a complex manner. One prediction of this hypothesis is that, just as mutations in cis are able to affect both PrP topology and development of disease, loss or inactivation of specific trans-acting factors might also alter PrP topology in favor of $C^{tm}PrP$ and potentiate development of neurodegeneration.

Once synthesized at the ER, $C^{tm}PrP$ is thought to exit to a post-ER compartment on the basis of the acquisition of resistance to digestion by endo H (Fig. 3B). We postulate that although exit from the ER can

occur in some instances, $C^{tm}PrP$ may normally be degraded before exit, a fate observed for some posttranslationally regulated proteins (33). This degradation may explain why the expression of any given PrP construct at the ER in the cell-free system results in a higher percentage of transmembrane PrP chains than were detectable for that construct in brain at steady state. The observation of a lack of $C^{tm}PrP$ accumulation in Tg[SHaPrP(KH \rightarrow II) $_{L}$] mice, despite readily detectable $secPrP$, supports this model.

At the present time, we do not know how $C^{tm}PrP$, upon exit from the ER, is able to cause disease. The correlation of three independent PrP mutants that promote $C^{tm}PrP$ synthesis in cell-free systems, with development of neurodegenerative disease in either transgenic mice or humans, and the detection of $C^{tm}PrP$ in brain suggest a causative role in disease. Whether inappropriately expressed $C^{tm}PrP$ is able to initiate specific signaling events to cause cell death or accomplishes this end by another mechanism remains to be determined. The pathway involving $C^{tm}PrP$ may not be the only

Fig. 7. A model for the role of $C^{tm}PrP$ in neurodegeneration. Nascent PrP is synthesized in the $secPrP$, $N^{tm}PrP$, or $C^{tm}PrP$ form. The $C^{tm}PrP$ form may subsequently be rapidly degraded in the ER or,



in some cases, may be able to escape degradation to a post-ER compartment. Upon exit from the ER, $C^{tm}PrP$ is proposed to cause disease. Whether the branch points that determine PrP topology and degradation can be regulated by trans-acting factors remains to be determined.

pathway of neurodegeneration, although it appears to be the one used in GSS(A117V), as demonstrated here. Recognition of C^{tm} PrP and its involvement in some cases of GSS should facilitate the biochemical identification of other steps in a putative signaling cascade. Proteins undergoing topological regulation like C^{tm} PrP may be involved in neurodegenerative diseases besides those currently attributed to prions.

REFERENCES AND NOTES

1. S. B. Prusiner, *Science* **278**, 245 (1997); C. Weissmann, *Prog. Brain Res.* **105**, 15 (1995).
2. S. Brandner et al., *Nature* **379**, 339 (1996).
3. H. Bueler et al., *Cell* **73**, 1339 (1993).
4. S. B. Prusiner et al., *Proc. Natl. Acad. Sci. U.S.A.* **90**, 10608 (1993).
5. D. A. Kocisko et al., *Nature* **370**, 471 (1994); S. B. Prusiner et al., *Cell* **63**, 673 (1990).
6. M. Scott et al., *Cell* **73**, 979 (1993).
7. J. Tateishi et al., in *Prion Diseases of Humans and Animals*, S. B. Prusiner, J. Collinge, J. Powell, B. Anderton, Eds. (Horwood, London, 1992), pp. 129–134; J. Collinge et al., *Lancet* **346**, 569 (1995); J. Tateishi et al., *Nature* **376**, 434 (1995); P. A. Hayward, J. E. Bell, J. W. Ironside, *Neuropathol. Appl. Neurobiol.* **20**, 375 (1994).
8. K. K. Hsiao et al., *Proc. Natl. Acad. Sci. U.S.A.* **91**, 9126 (1994).
9. J. C. Manson, A. R. Clarke, P. A. McBride, I. McConnell, J. Hope, *Neurodegeneration* **3**, 331 (1994); H. Bueler et al., *Mol. Med.* **1**, 19 (1994).
10. B. Hay, R. A. Barry, I. Lieberburg, S. B. Prusiner, V. R. Lingappa, *Mol. Cell. Biol.* **7**, 914 (1987).
11. B. Hay, S. B. Prusiner, V. R. Lingappa, *Biochemistry* **26**, 8110 (1987).
12. C. S. Yost, C. D. Lopez, S. B. Prusiner, R. M. Myers, V. R. Lingappa, *Nature* **343**, 669 (1990).
13. C. D. Lopez, C. S. Yost, S. B. Prusiner, R. M. Myers, V. R. Lingappa, *Science* **248**, 226 (1990).
14. N. Stahl, D. R. Borchelt, K. K. Hsiao, S. B. Prusiner, *Cell* **51**, 229 (1987).
15. G. Blobel and B. Dobberstein, *J. Cell Biol.* **67**, 852 (1975); F. N. Katz et al., *Proc. Natl. Acad. Sci. U.S.A.* **74**, 3278 (1977); D. Shields and G. Blobel, *J. Biol. Chem.* **253**, 3763 (1978).
16. B. Oesch et al., *Cell* **40**, 735 (1985).
17. K. A. De Fea et al., *J. Biol. Chem.* **269**, 16810 (1994).
18. R. S. Hegde et al., unpublished data.
19. R. Riek et al., *Nature* **382**, 180 (1996).
20. T. L. James et al., *Proc. Natl. Acad. Sci. U.S.A.* **94**, 10086 (1997).
21. D. G. Donne et al., *ibid.*, p. 13452.
22. D. Westaway et al., *Cell* **76**, 117 (1994).
23. M. R. Scott et al., *Protein Sci.* **6** (suppl. 1), 84 (1997).
24. W. J. Welch, J. I. Garrels, G. P. Thomas, J. J. Lin, J. R. Feramisco, *J. Biol. Chem.* **258**, 7102 (1983).
25. D. N. Hebert, B. Foellmer, A. Helenius, *Cell* **81**, 425 (1995).
26. K. K. Hsiao et al., *Neurology* **41**, 681 (1991); J. A. Mastrianni et al., *ibid.* **45**, 2042 (1995); C. Tranchant et al., *J. Neurol. Neurosurg. Psychiatry* **55**, 185 (1992).
27. J. Tateishi et al., *Neurology* **40**, 1578 (1990).
28. J. A. Mastrianni et al., unpublished data.
29. M. E. Mathieu, P. R. Grigera, A. Helenius, R. R. Wagner, *Biochemistry* **35**, 4084 (1988); W. J. Ou, J. J. Bergeron, Y. Li, C. Y. Kang, D. Y. Thomas, *J. Biol. Chem.* **270**, 18051 (1995).
30. K. Hsiao et al., *Nature* **338**, 342 (1989).
31. J. Tateishi and T. Kitamoto, *Brain Pathol.* **5**, 53 (1995).
32. T. Muramoto et al., *Nature Med.* **3**, 750 (1997).
33. S. Wang, R. S. McLeod, D. A. Gordon, Z. Yao, *J. Biol. Chem.* **271**, 14124 (1996); J. S. Bonifacino et al., *Nature* **344**, 247 (1990).
34. R. S. Hegde and V. R. Lingappa, *Cell* **85**, 217 (1996).
35. D. Serban, A. Taraboulos, S. J. DeArmond, S. B. Prusiner, *Neurology* **40**, 110 (1990).
36. H. Schagger and G. von Jagow, *Anal. Biochem.* **166**, 368 (1987).
37. M. R. Scott et al., *Protein Sci.* **1**, 986 (1992).
38. K. K. Hsiao et al., *Science* **250**, 1587 (1990).
39. For cell-free translation of PrP and mutants, each coding region was engineered into an sp64 plasmid vector containing the SP6 promoter followed by the 5' untranslated region of Xenopus globin. Transcription with SP6 polymerase, translation in rabbit reticulocyte lysate containing microsomal membranes from dog pancreas, and proteolysis were done as described previously [(34), and references therein]. All translation reactions were carried out at 32°C for 60 min and proteolysis reactions at 0°C for 60 min with PK (0.5 mg/ml). Products were immunoprecipitated with either the 3F4 mAb (Fig. 1, D and E) or R073 antibody (Fig. 1F) (35) and analyzed by 10% tricine-SDS-PAGE (36), and the proteins were visualized by autoradiography.
40. M. Rogers et al., *J. Immunol.* **147**, 3568 (1991).
41. Relative amounts of the topological forms of PrP were quantitated by densitometry of the three products resulting after protease digestion in the absence of detergent: full-length, undigested PrP (sc PrP), the 18-kD COOH-terminal fragment (C^{tm} PrP), and the 14-kD NH₂-terminal fragment (N^{tm} PrP). Densitometric values for COOH- and NH₂-terminal fragments were adjusted (to compensate for loss of radioactivity due to proteolytic digestion of a portion of the molecule) to obtain quantitative estimates of C^{tm} PrP and N^{tm} PrP.
42. For transgenic mice production, PrP coding regions were engineered into the cosShA.Tet cosmid expression vector (37) at the Sal I site. cosShA.Tet cosmids containing the appropriate PrP transgenes were digested with Not I, and the transgene was purified and used for microinjection into the pronuclei of fertilized FVB/Prnp^{0/0} oocytes as previously described (38). We assessed the presence of the transgene in weanling animals by screening genomic DNA isolated from tail tissue with a probe specific to the 3' untranslated region of the SHaPrP gene contained in the cosShA.Tet vector. PrP expression was assessed by immunoblotting of brain tissue homogenate with 13A5 mAb, comparing this tissue with serial dilutions of normal Syrian hamster brain tissue (see Fig. 2C for an example). Levels of expression (relative to normal hamster) of each transgenic line are shown in Table 1.
43. Microsomal membranes were isolated from fresh brain tissue after homogenization in about 20 volumes of ice cold buffer [0.25 M sucrose, 100 mM KCl, 5 mM MgAc₂, 50 mM Hepes (pH 7.5), and 0.5 mM phenylmethylsulfonyl fluoride (PMSF)] by successive passage, five times each, through 16-, 18-, 20-, and 22-gauge needles. Homogenate was centrifuged for 10 min at 12,000g at 4°C. Supernatant was removed and centrifuged for either 20 min at 100,000 rpm in TLA-100.3 rotor (Beckman) or 60 min at 65,000 rpm in 70.1Ti rotor (Beckman). Supernatant was discarded and pellet resuspended in the same buffer as above, but without PMSF, at a concentration of 500 μl per gram of starting tissue. Topology was assessed by digestion of membranes with PK as described (39), followed by digestion with PNGase as directed by the manufacturer (New England Biolabs). Samples were precipitated with trichloroacetic acid, separated by 10% tricine-SDS-PAGE, transferred to nitrocellulose, and probed with either 3F4 or 13A5 mAb as indicated in the figure legends.
44. R. S. Hegde et al., data not shown.
45. G. C. Telling et al., *Science* **274**, 2079 (1996).
46. Brain tissue (frozen) was homogenized in phosphate-buffered saline (PBS) (at 5% w/v or 10% w/v) by successive passage through 16-, 18-, and 20-gauge needles. Cell-free translation reactions were assayed directly. For C^{tm} PrP detection ("mild" proteolysis conditions), portions of the sample were adjusted to 1% NP-40 and PK (0.25 mg/ml) (Merck) and incubated for 60 min on ice. For PrP^{Sc} detection ("harsh" proteolysis conditions), samples were adjusted to 0.5% NP-40, 0.5% deoxycholate, and PK (0.1 mg/ml) and incubated for 60 min at 37°C. The difference between mild and harsh digestion conditions, although operational, is not subtle, as it involves a 37° change in temperature of incubation and the presence of nonionic detergent compared with mixed micelles of nonionic and ionic detergents. Detailed characterization of the relative contributions of each of these parameters to detection of C^{tm} PrP will be reported elsewhere (28). The proteolysis reactions were terminated by adding PMSF to 5 mM, incubating an additional 5 min, and transferring the sample to 5 volumes of boiling 1% SDS and 0.1 M Tris (pH 8.9). Brain-derived samples were then digested with PNGase as directed by the manufacturer, resolved by 10% tricine-SDS-PAGE, transferred to nitrocellulose, and probed with either the 3F4 (Fig. 6B) or 13A5 (Fig. 6A) mAb. In vitro translation products (Fig. 5A) were immunoprecipitated with 3F4 and analyzed by SDS-PAGE and autoradiography.
47. We thank J. Cayetano for help with the histopathology; A. Calayag, O. Nguyen, and R. Köhler for technical assistance; R. Cotter and C. Petromilli for animal care; H. Serban for reagents; G. Telling for advice; and J. Taltzelt, R. Nixon, S. Russel, and J. Lingappa for stimulating discussions. Supported by NIH grant AG02132 and the Medical Scientist Training Program.

29 October 1997; accepted 24 December 1997

Make a quantum leap.

SCIENCE Online can help you make a quantum leap and allow you to follow the latest discoveries in your field. Just tap into the fully searchable database of SCIENCE research abstracts and news stories for current and past issues. Jump onto the Internet and discover a whole new world of SCIENCE at the Web address:

www.sciencemag.org

SCIENCE